MUD PUMP PRESSURE PULSATION CONTROL SYSTEMS

MIHAEL CIPEK, DANIJEL PAVKOVIĆ, JURAJ BENIĆ, ŽELJKO ŠITUM

University of Zagreb, Faculty of Mechanical Engineering and Naval Architecture, Croatia
mihael.cipek@fsb.hr, danijel.pavkovic@fsb.hr, juraj.benic@fsb.hr, zeljko.situm@fsb.hr

Drilling fluid is circulated through the well-bore during drilling operations to transport cuttings from the bottom of the hole to the surface. Hydrostatic high-pressure mud pumps are typically used for this purpose. Triplex pumps, which comprise three pistons mechanically displaced by 120 degrees, are the most common type of mud pump. When more than one mud pump is connected to the common high-pressure line, very high pressure peaks can occur due to asynchronous pump strokes. These pressure peaks can damage high-pressure mud lines and pressure equipment, such as valves and gaskets. They can also undermine well-bore stability. This paper investigates the process of pulsation creation and proposes adequate pressure control systems for pulsations reduction. The proposed systems are based on the use of passive and active control elements.

Keywords:
mud pump, drill-string, drilling fluid, pressure pulsations, pressure control

University of Maribor Press

DOI https://doi.org/10.18690/um.fs.5.2023.18
ISBN 978-961-286-781-2

1 Intruduction

Deep drilling operations are required to produce deep wells for the exploitation of hydrocarbons or geothermal energy [1]. A drilling fluid (also called drilling mud) circulating through the well-bore is crucial for this process. Its main purpose is to transport cuttings from the bottom of the hole to the surface through the annulus between the borehole walls and the drill-string. Mud is also used to control the pressure within the well. In particular, the mud pressure must be higher than the well pressure to avoid accidental blowouts, which can have potentially severe consequences for personnel, equipment, and the environment. The mud pressure must also be sufficiently low to avoid accidental fracturing of the well [2].

Mud pumps are used to circulate drilling mud through the well-bore. They are typically reciprocating piston devices, with triplex pumps being the most common type [3]. Triplex pumps have three pistons that are mechanically displaced by 120 degrees [4]. When more than one mud pump is connected to the common high-pressure line, high pressure peaks can occur due to asynchronous pump strokes. These pressure peaks can damage high-pressure mud lines and pressure equipment, such as valves and gaskets. They can also undermine well-bore stability.

One way to reduce these harmful high pressure spikes is to control the phase displacement of individual pumps with respect to each other. This can be done by synchronizing the timing of pump strokes, which leads to equal peak amplitudes. For example, if only one triplex mud pump is connected to a single high-pressure line, there is no possibility of high pressure peaks since all three pistons are mechanically displaced by 120°. However, if two or more triplex pumps are connected to a single high-pressure line, pressure peaks are likely to occur. The dynamics of this system are chaotic, and the angular phase differential between two pumps may be considered quasi-random. This means that there is a much higher probability for pressure peaks to occur in this case [2].

This paper conducts the analysis of pulsation creation and proposes an adequate pressure control systems for pulsations reduction. The proposed systems are based on the use of passive and active control elements.

2 Mud pump system mathematical model

A mud pump is a positive displacement machine consisting of two or more cylinders, each containing a piston or a plunger, which are driven through respective slider-crank mechanisms and a common crankshaft powered by an external source. Rotational speed of the crankshaft, and the number of pistons and their respective dimensions determine a pump capacity. Unlike a centrifugal pump, a positive displacement pump does not develop pressure; it only produces a flow of fluid. The downstream process or piping system produces a resistance to this flow, thereby generating pressure in the piping system and the discharge portion of the pump [5]. Pump flow fluctuates at a rate proportional to the pump speed and the number of cylinders. The amplitude of these fluctuations is a function of the number of cylinders. Generally speaking, the greater the number of cylinders, the lower the amplitude of the flow variations at a specific rotational speed. Mud pumps are capable of producing a variable capacity when coupled to a variable speed drive. Each pump has maximum suction and discharge pressure limits that, when combined with its maximum speed, determine the pump's power rating.

The pump can be subjected to power inputs that are less than its maximum rating, which only results in a slight decrease of its mechanical efficiency. In a positive displacement pump, when pressure exceeds the design limits of the pump, mechanical failure (often catastrophic) may occur unless excess pressure is quickly relieved. For this reason, all piping systems incorporating positive displacement pumps must have discharge pressure relief devices to limit the pressure in the piping system and to avoid pump failure [5].

2.1 Kinematics of piston movement

Mud pump kinematics can be described by a simple slider-crank mechanism. By applying a Cosine law for the aforementioned mechanism, the position of plunger pin from crank shaft centre (corresponds to plunger position) X can be described as:

$$X = r + L - r\cos\theta_{cs} - \sqrt{L^2 - r^2\sin^2(\theta_{cs})} \tag{1}$$

where r is the radius of the crank shaft, L is the length of the connecting rod, and θ_{cs} is crank shaft angle. Crankshaft angle is calculated from crankshaft speed ω_{cs} as follows:

$$\theta_{cs} = \int \omega_{cs}\, dt \tag{2}$$

2.2. Isothermal pressure drop

Drilling fluid is compressed within pump cylinders. Volume inside the pump cylinder consists of the dead volume V_0 (volume when plunger is in its top dead centre position) and the changeable (variable) volume ΔV_a which is directly determined by the plunger position ΔX. This volume can be defined as follows:

$$\Delta V_c = V_0 + \Delta V_a = V_0 + \frac{D^2\pi}{4}\Delta X, \tag{3}$$

where D is diameter of the plunger. Overall cylinder volume in the top dead centre position is $V_{c,\min} = V_0$, while in the bottom dead centre position, the total volume is given by the following straightforward relationship:

$$V_{c,max} = V_0 + \frac{D^2\pi}{4} 2r. \tag{4}$$

On the other hand, the relationship between isothermal pressure drop dp and changeable volume dV is described by compressibility coefficient β, defined as [6-8]:

$$\beta = -\frac{dV}{dp} \cdot \frac{1}{V_{c0}}, \tag{5}$$

where V_{c0} refers to the initial chamber volume.

By applying expression (5) to the volume inside the mud pump cylinder, the pressure drop inside any cylinder (denoted by cylinder number n) can be described as:

$$dp_{c,n} = -\frac{dV_n}{\beta V_{c,n}}, \tag{6}$$

where

$$dV_n = \frac{D^2\pi}{4} dX_n, \tag{7}$$

and $V_{c,n}$ corresponds to the n^{th} cylinder initial volume (at compression starting point).

2.3 Simplified drilling fluid hydraulic circuit

Figure 1 shows the simplified hydraulic circuit of the drilling fluid, which includes the compression of fluid volumes V_{c1}, V_{c2}, V_{c3} inside each of the n = 3 cylinders, fluid volume inside the drill string V_{ds}, pressure drop within the drill string Δp_{Dr}, and flow dynamics through the check valves. Figure 1 also shows the mechanical part of the mud pump mechanism. Three pump cylinders are mechanically coupled by a crank shaft (each separated by a $360°/n$ = 120° degree angle). Electric motor(s) propel the crankshaft through power transmission chain and gear with i_{belt} and i_g ratios, respectively.

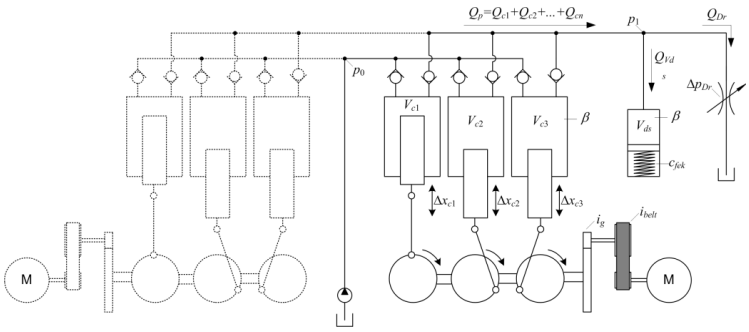

Figure 1: Principal schematic representation of simplified mud hydraulic cycle.
Source: own.

Volumetric fluid flow rate is defined as follows [6]:

$$Q = \frac{dV}{dt}. \tag{8}$$

Volume of the drill string $V_{ds} = l\pi D_{ds}^2/4$ (where l is drill-string length, D_{ds} is its inner diameter) in Fig. 1 is represented as a single chamber, where chamber input/output flow Q_{Vds} can be calculated as the difference of the overall pumping flow Q_p and Q_{Dr} (Q_{Vds}=Q_p – Q_{Dr}). Therefore, the pressure drop dp_1 is defined as:

$$dp_1 = -\frac{1}{\beta V_{ds}}\left(Q_p - Q_{Dr}\right)dt. \tag{9}$$

The bore-hole flow (flow through the drill string) is concentrated within the drilling tool (drill bit) and it is simply represented as a damping (valve) element which can be mathematically described as:

$$Q_{Dr} = K_{Dr}A_{Dr}\sqrt{\Delta p_{Dr}}, \tag{10}$$

where A_{Dr} is cross section area of the flow hole (orifice area). K_{Dr} is damping coefficient which includes mass density of fluid ϱ and the coefficient of discharge for the orifice a_D [20]:

$$K_{Dr} = \alpha_D\sqrt{\frac{2}{\rho}}. \tag{11}$$

Due to the variability and uncertainty of A_{Dr}, a_D and ϱ parameters of the drilling process, they are approximated and lumped together within a fixed parameter $1/k_{ds}$. Following from that, the flow Q_{Dr} can be expressed as:

$$Q_{Dr} = k_{ds}\sqrt{\Delta p_{Dr}}. \tag{12}$$

Fluid flow through check valves can be represented in the form similar to Eq. (10). The high-pressure check valve (discharge valve) within the pumping mechanism is open only if the cylinder pressure $p_{c,n}$ is larger than the pressure inside the drill string (p_1), which gives the following relationship for the check valve flow rate:

$$\begin{aligned} Q_{c,n} &= k_{cv}\sqrt{p_{c,n} - p_1} \quad \text{for} \quad p_{c,n} > p_1 \\ Q_{c,n} &= 0 \qquad\qquad\qquad\quad \text{otherwise}, \end{aligned} \tag{13}$$

where k_{cv} is the lumped damping parameter of the valve. Similar relationship is valid for the low pressure check valve (intake valve). Namely, it is open only if pressure within the cylinder $p_{c,n}$ is lower than the pressure inside intake manifold p_0 (charging pump pressure [9]):

$$Q_{i,n} = k_{cv}\sqrt{p_0 - p_{c,n}} \quad \text{for} \quad p_0 > p_{c,n}$$

$$Q_{i,n} = 0 \qquad \text{otherwise.} \tag{14}$$

While check valves are open the volume of the fluid inside the cylinder changes due to the fluid flow into each cylinder according to:

$$V_{f,n} = \int (Q_{i,n} - Q_{c,n}) dt. \tag{15}$$

Therefore, the cylinder volume changes from $V_{c,n}$ to the following value:

$$V_{cc,n} = V_{c,n} + V_{f,n} \tag{16}$$

wherein the pressure inside the cylinder is $p_{c,n} \approx p_1$ in the case of discharge, while $p_{c,n} \approx p_0$ is valid in the case of intake.

Overall pump discharge flow is given as $Q_p = Q_{c,1} + Q_{c,2} + Q_{c,3}$, while the intake flow is $Q_{ia} = Q_{i,1} + Q_{i,2} + Q_{i,3}$. In the case of additional pumps connected to the same pipeline, pressure p_1 is equal for each pump, while flows of all pumps are added together $Q_{p,all}=Q_{p1}+Q_{p2}+\ldots+Q_{pn}$.

2.4 Mechanical relationships

Mechanical torque produced by the pressure $p_{c,n}$ inside each of the cylinders, and transferred to the crank shaft can be expressed as [10]:

$$m_{c,n} = p_{c,n} \frac{\pi D^2}{4} r \sin(\theta_{cs,n})(1 + \frac{r}{L} cos(\theta_{cs,n})). \tag{17}$$

The corresponding electrical motor torque required to maintain the pumping action can be calculated as follows:

$$m_l = J_{all} \dot{\omega}_m + \frac{\sum_{n=1}^{3} m_{c,n}}{i_{belt} i_g}, \tag{18}$$

where $\sum_{n=1}^{3} m_{c,n}$ overall crank shaft torque stemming from the in-cylinder pressure, J_{all} is lumped inertia of crankshaft J_{cs}, drive shaft J_{ds} and motor J_m and can be calculated as:

$$J_{all} = \frac{\frac{J_{cs}}{i_g^2} + J_{ds}}{i_{belt}^2} + J_m. \tag{19}$$

Table 1: Physical parameters of mud pump system.

L [m]	r [m]	D [m]	i_g	i_{belt}	V_0 [m³]
1.28	0.3048	0.14605	3.439	2.3384	0.006
β [Pa^{-1}]	k_{ds}	k_{cv}	J_{cs} [kgm²]		J_{ds} [kgm²]
45.8·10^{-11}	1.3·10^{-5}	0.0004	585.77		34.355

3 Triplex mud pump simulation models

This section presents the simulation models of the individual mud pumps and the overall triplex multiple pump system, implemented within the Matlab/Simulink™ software environment.

3.1 Slider-crank mechanism (Cylinder) sub-model

Figure 2 shows the block diagram of the slider-crank mechanism (Cylinder) sub-model while the corresponding simulation model is implemented within Matlab/Simulink™ software environment. According to mathematical model described above, volume change ΔV_c in the cylinder occurs due to plunger movement, which is calculated by integrating the crank-shaft speed ω_{cs} from the starting angle θ_{cs0}.

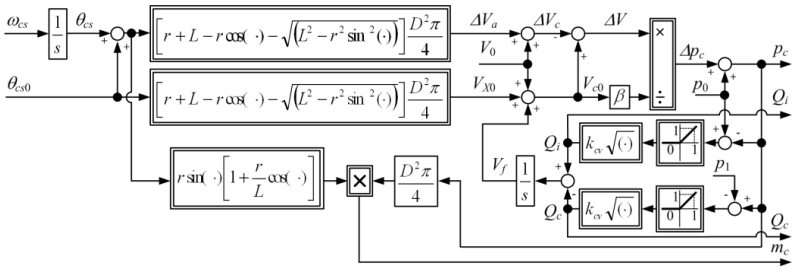

Figure 2: Block diagram representation of Cylinder sub-model
Source: own.

While check valves are closed, overall volume change within the cylinder ΔV is equal to ΔV_c, and the pressure changes according to pressure drop Δp_c relationship. On the other hand, when the cylinder pressure p_c is larger than the pressure inside the

drill string p_1, the high-pressure check valve (discharge valve) opens, which initiates the fluid flow Q_c, and results in a decrease of the fluid volume inside the cylinder by V_f. Finally, when the cylinder pressure p_c is lower than the pre-charge pressure p_0, the low-pressure check valve (intake valve) opens, which results in fluid flow Q_i into the cylinder, and consequent increase of the fluid volume inside the cylinder by V_f.

3.2 Triplex mud pump and drill string pipeline hydraulic system simulation model

Figure 3. shows the block diagram of the triplex mud pump hydraulic system model together with the drill-string pipeline model. Within the triplex mud pump model, the three individual pump pistons are mechanically coupled by a crank shaft (each separated by a $360°/n = 120°$ degree angle). The overall crank shaft torque is the sum total of all cylinder torques $m_{cs} = m_{c,1} + m_{c,2} + m_{c,3}$. Intake and discharge flows of each cylinder are hydraulically coupled, which means that the pump discharge flow is the sum total of all cylinder discharge flows $Q_p = Q_{c,1} + Q_{,c,2} + Q_{c,3}$, and pump intake flow is the sum total of all cylinder intake flows $Q_{ia} = Q_{i,1} + Q_{i,2} + Q_{i,3}$. On the other hand, pre-charge pressure p_0, and drill string pressure p_1 are the same for each cylinder.

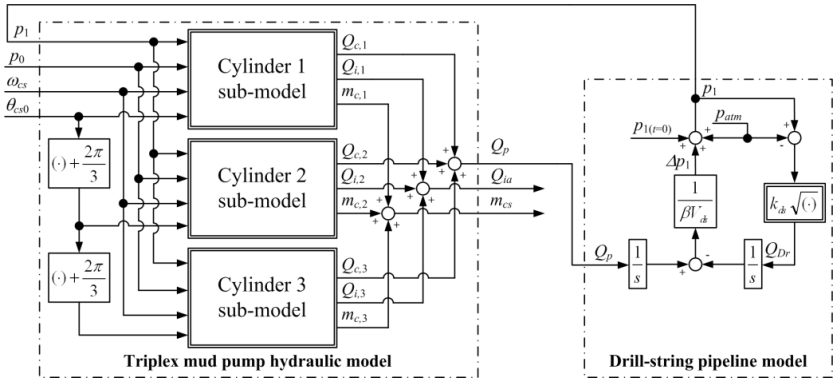

Figure 3: Block diagram representation of Triplex mud pump hydraulic and Drill-string pipeline model.

Source: own.

Moreover, within the drill-string pipeline model, fluid volume inside the pipeline $V_{ds} = l \times \pi D^2/4$ (l is pipeline length, D is pipeline cross section) is represented by a single chamber, wherein chamber input/output flow can be calculated as the difference of

the overall pumping flow Q_p and bore-hole flow Q_{Dr} (flow through the drill string channelled into the borehole through the drilling tool). Analogously, the volume difference inside the pipeline can be calculated by integrating the flow difference. Finally, based on the aforementioned relationships, the drill string pressure p_1 is then built up due to the volume difference, which is described by well-known pressure drop relationships (see section 2.3). Naturally, atmospheric pressure p_{atm}, and initial drill string pressure $p_{1(t=0)}$ can be included within the drill string model as well, as freely configurable parameters, or as input variables.

3.3 Overall triplex mud pump model

The overall simulation model of the triplex mud pump system, built up from previously described sub-models is shown in Fig. 4, within the framework of speed-controlled DC electrical drive featuring a speed/current cascade control system [11]. The motor controller parameters are determined according to the damping optimum criterion. Block diagram (Fig. 4.) also shows that the motor speed reference ω_{mref} is determined by multiplying the requested pump speed reference ω_{pref} with i_{belt} and i_g power transmission ratios. Negative load torque m_l (crank shaft torque reduced by power transmission ratios $m_l=m_{cs}/i_{belt}i_g$) is added to the motor torque, and the resulting torque difference accelerates the total inertia J_{all} (equation (19)) with the angular acceleration rate $\dot{\omega}_m$, which is used within the model to obtain the motor speed ω_m through integrating the angular acceleration $\dot{\omega}_m$. Pump crank shaft speed is then calculated as motor speed reduced by the overall transmission ratio ($\omega_{cs} = \omega_m/i_{belt}i_g$).

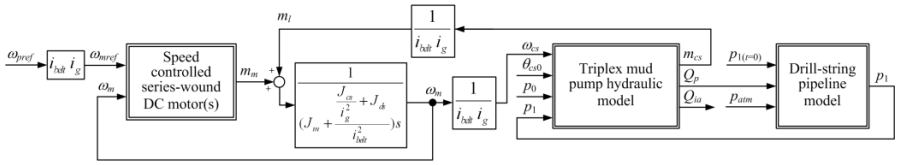

Figure 4: Block diagram of overall triplex mud pump model.

Several independent mud pump models described above can be easily incorporated into an extended multiple pump. In the case when an additional pump is added, intake and discharge flows of all connected pumps are summed together ($Q_{p,all}=Q_{p,1}+Q_{p,2}+\ldots+Q_{p,n}$ and $Q_{ia,all}=Q_{ia,1}+Q_{ia,2}+\ldots+Q_{ia,n}$) while the drill string pressure p_1 and pre-charge pressure are still equal for each pump, respectively.

4 Pressure pulse analysis

Previously defined model of two interconnected mud pumps is simulated for the case of speed reference ω_{cs} of 120 strokes per minute (SPM) and initiating phase angle of first (Master) pump of $\theta_{cs0} = 0$ degrees, while the second (Slave) pump initiating angle has been varied within the range $\omega_{cs1} = 0…120$ degrees with 1° increment. Figure 5 shows the pressure pulsation steady-state magnitudes from simulations dependent on the pump phase displacement (crank shaft angle between two pumps). Each sub-plot (Fig 5a-d) represents the results for different amounts of fluid volume inside the drill string V_{ds} (different hydraulic compliance of the system). These results show that the pressure pulsation magnitude generally decreases as the drill string fluid volume capacity increases, and that for the all considered cases the drill string pressure pulsations may be notably reduced if second pump is shifted in phase by 30° or 90°.

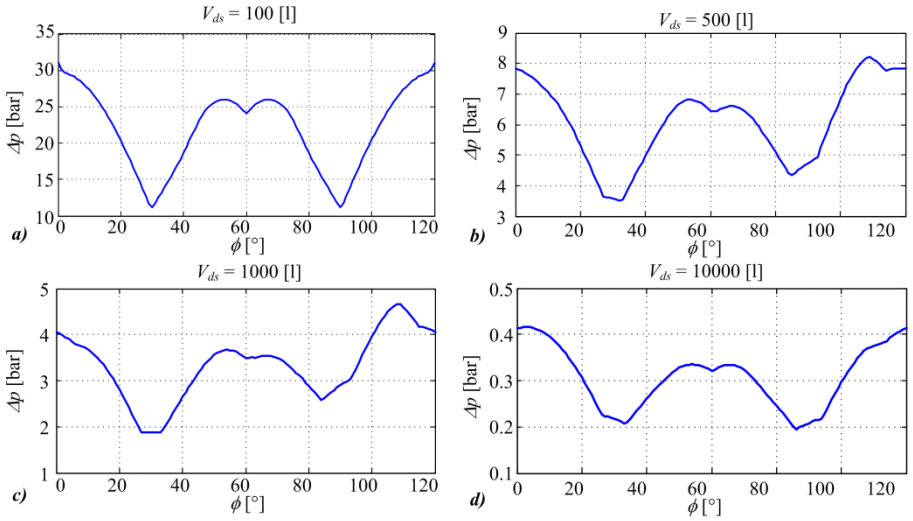

Figure 5: Simulation responses of pressure oscillations for drill-string volume: 100 L (a), 500 L (b), 1000 L (c), and 10000 L (d).

Source: own.

Similar approach to pressure pulsation analysis can be used for the case of three interconnected mud pumps. Again, simulations were carried out for the case of speed reference ω_{cs} of 120 strokes per minute (SPM) and initiating angle of first pump (Master pump) being $\theta_{cs0} = 0$ degrees. The other two pumps have had the

initiating phase angle within the range $\theta_{cs1,2}$ = 0 … 120 degrees (with 2 degree increments for each point). Simulation results presented in Fig. 6 indicate that pressure pulsations magnitude depends on phase shifts of both auxiliary pumps, and there appear to be eight possible combinations of phase shifts which result in minimal pressure pulsations.

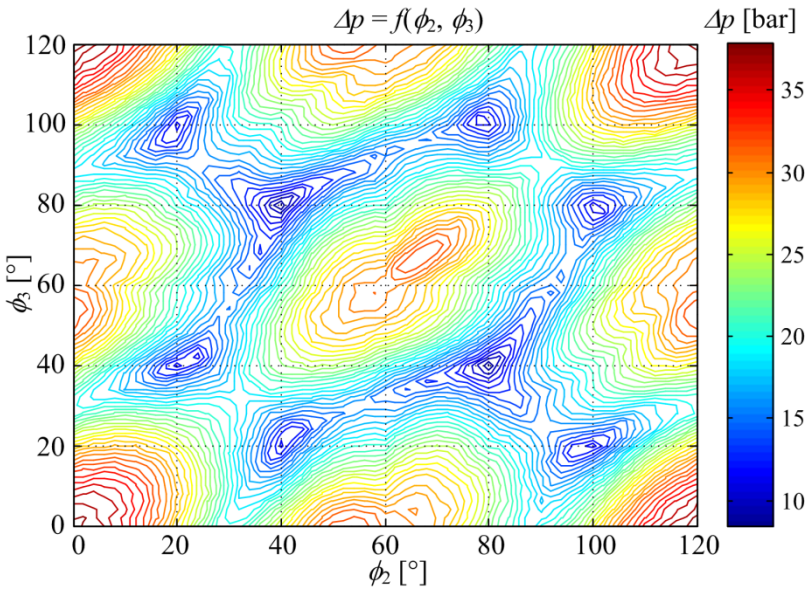

Figure 6: Simulation responses of pressure oscillations for 100 L drill-string volume and three mud pumps

Source: own.

5 Mud pump control system concept

The mud pump control system concept is based on above pressure pulsation analysis for the case of two and three interconnected triplex mud pumps. The pump phase shift controller, shown in Figure 7, uses integrators to measure time intervals between the SPM pulses from the master and slave pumps, while also considering the pump speed reference in order to calculate the phase shift between the master and slave pump. The phase shift result is subtracted from the "optimal" pump phase displacement reference, and the resulting error is multiplied by a proportional gain k_{adhoc}. To avoid possible phase shift overshoots, a saturation block has been also included within the controller, whose output represents the speed reference bias $\Delta\omega$, which is added to the speed reference of the slave pump. The controller is extended

by additional rule which utilizes the fact that the angle difference between each piston each stroke amounts to 120° for the considered triplex mud pump. So, for the case when controller estimated phase angle is larger than 120°, this additional rule adds an 120° offset to the phase reference. This additional rule can also be applied in the same way for the phase angle larger than 240°.

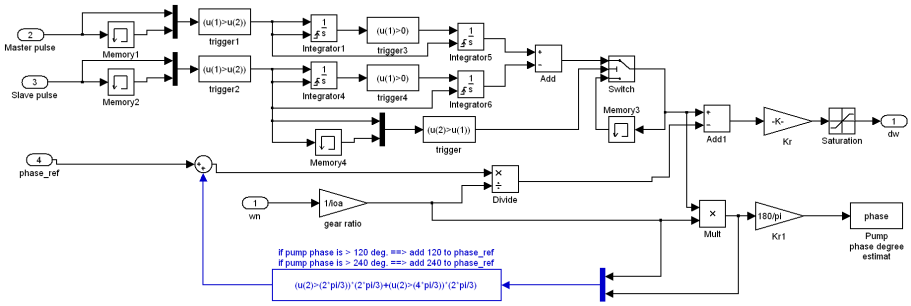

Figure 7: Matlab/Simulink™ representation of simple phase controller.
Source: own.

It is assumed that both pumps are equipped with Stroke Per Minute (SPM) sensor which gives one pulse per one crank shaft revolution, and that electrical motors driving the pumps are also equipped with fast (stiff) embedded speed controller. The above control system can also be applied to three interconnected mud pumps and the drill-string system, as shown in Figure 8.

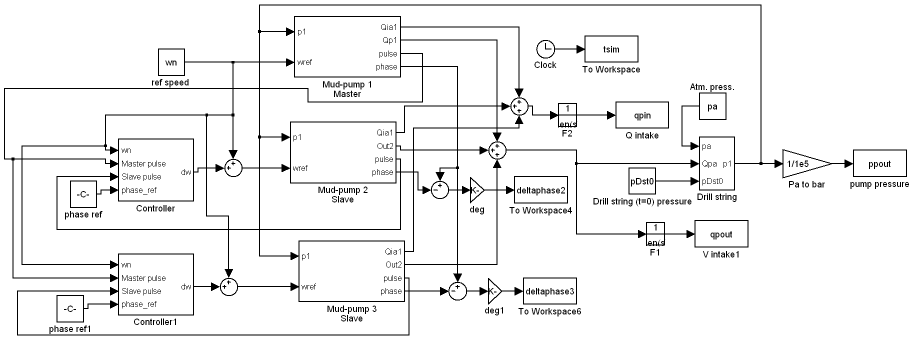

Figure 8: Matlab/Simulink™ implementation of overall "soft-pump" control system of three triplex mud pumps.
Source: own.

In that case, the proposed system possesses two separate phase shift controllers for each slave pump. Each slave pump controller calculates the phase angle of slave pump reference to the master pump angle.

5.1 Simulation results

Figure 9 shows the simulation results of the phase-controlled three mud pump system, with the pumps speed reference ω_{pref} set to 120 SPM ($\theta_{cs0} = 0°$), and the initial drill string pressure set to atmospheric pressure value of 1 bar.

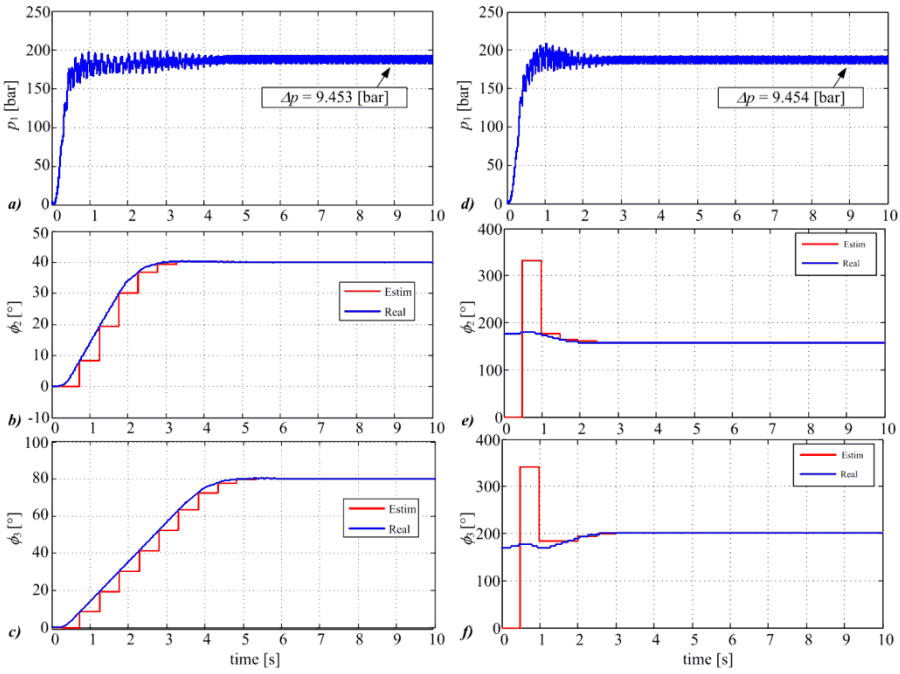

Figure 9: Simulation responses of soft mud pump: pressure (a) and phase of first slave (b) and second slave (c) for all pump starts from 0°, and pressure (d) and phase of first slave (e) and second slave (f) for slave pumps starts phase displaced by 180°.

Left-hand-side sub-plots (Figs. 9a-c) show the simulation responses in the case when slave pumps start in phase with the master ($\theta_{cs1} = 0°$), while right-hand-side sub-plots (Fig. 9d-f) show the case when slave pumps start with half turn phase advance ($\theta_{cs1} = 180°$) with respect to the master pump. For both scenarios, the phase displacement between pumps is brought to the desired (reference) values which correspond to minimal pressure pulsations.

6 Conclusion

Three-piston (triplex) mud pump simulation models are presented and simulated in this study. The simulation results illustrate the dominant flow and pressure pulsation phenomena. The pressure pulsation and phase displacement analyses for the case of two interconnected three-piston (triplex) mud pumps have shown that minimal pressure pulsations occur when master and slave pumps are phase-shifted by a 30° or 90° angle, while in the case of three interconnected pumps, the analysis has shown that eight distinct combinations of phase shifts between individual pumps result in minimum pressure pulsation magnitude. The mud pump pressure pulsation control system concept has also been presented in this study. The proposed controller adjusts the speed reference of the slave pump in order to achieve the required phase shift of 30 degrees for two pumps, while several different combinations are possible for three interconnected pumps in order to achieve the minimum pressure pulsation magnitude.

Acknowledgments

It is gratefully acknowledged that the technological R&D presented in this work has been supported by the Croatian Agency for SMEs, Innovations and Investments (HAMAG-BICRO) through the collaborative R&D grant Advanced Systems for Drilling Control at Hydrocarbon Exploration Facilities (grant No. IR-2015-48), and by several technological R&D projects financed by HELB Ltd. This research has also been supported by the European Regional Development Fund under the grant KK.01.1.1.01.0009 (DATACROSS).

References

[1] Pavković, D., Šprljan, P., Cipek, M., Krznar, M.(2021). Cross-axis control system design for borehole drilling based on damping optimum criterion and utilization of proportional-integral controllers. *Optimization and Engineering*, 22, pp 51–81. doi:10.1007/s11081-020-09566-z

[2] Pavković, D. Current Trends in Oil Drilling Systems R&D with Emphasis on Croatian Oil Drilling Sector – A Review, *Proceedings of the 9th International Conference on Management of Technology – Step to Sustainable Production* (MOTSP 2017), Dubrovnik, Croatia, 2017.

[3] Guo, B., Lui, G., (2011). Chapter One - Equipment in Mud Circulating Systems, Applied *Drilling Circulation Systems - Hydraulics, Calculations and Models,* pp 3-18. doi:10.1016/B978-0-12-381957-4.00001-2

[4] National Oilwell Varco: Mud Pumps - 14-P-220 Triplex Pumps, Technical Marketing Sheet, 2016.

[5] Karassik, I.J., Messina, J.P., Cooper, P., Heald, C.C.(2008). *Pump Handbook*, 4th ed., The McGraw-Hill Companies, Inc.

[6] Lewis, E.E., Stern, H. (1962). *Design of Hydraulic Control Systems*, The McGraw-Hill Companies, Inc.

[7] Wilson, D.R., Campbell, M.E., Breed, L.W., Hass, H.S., Galate, J. (1971). *Engineering Design Handbook, Hydraulic Fluids*, Headquarters, U.S. Army Materiel Command.

[8] Helduser, S. (1998). *Hydraulik und Pneumatik Übungsaufgaben*, Technische Universität Dresden.

[9] Collier, S.L. (1983). *Mud Pump Handbook*, Gulf Publising Company, Huston.
[10] Nigus, H. (2015). Kinematics and Load Formulation of Engine Crank Mechanism. *MMSE Journal – Mechanics, Materials Science & Engineering*, ISSN 2412-5954.
[11] Leonhard, W. (1987). *Control of Electrical Drives*, 1st ed., Springer-Verlag, Berlin.
[12] Schröder, D. (2007). *ElektrischeAntriebe - Regelung von Antriebssystemen*, 3rd ed., Springer-Verlag, Berlin.